AMERICAN SOCIETY FOR MICROBIOLOGY | Journal of Bacteriology®

RESEARCH ARTICLE

Mutational Activation of Antibiotic-Resistant Mechanisms in the Absence of Major Drug Efflux Systems of *Escherichia coli*

Hyunjae Cho,[a] Rajeev Misra[a]

[a]School of Life Sciences, Arizona State University, Tempe, Arizona, USA

ABSTRACT Mutations are one of the common means by which bacteria acquire resistance to antibiotics. In an *Escherichia coli* mutant lacking major antibiotic efflux pumps AcrAB and AcrEF, mutations can activate alternative pathways that lead to increased antibiotic resistance. In this work, we isolated and characterized compensatory mutations of this nature mapping in four different regulatory genes, *baeS*, *crp*, *hns*, and *rpoB*. The gain-of-function mutations in *baeS* constitutively activated the BaeSR two-component regulatory system to increase the expression of the MdtABC efflux pump. Missense or insertion mutations in *crp* and *hns* caused derepression of an operon coding for the MdtEF efflux pump. Interestingly, despite the dependence of *rpoB* missense mutations on MdtABC for their antibiotic resistance phenotype, neither the expression of the *mdtABCD-baeSR* operon nor that of other known antibiotic efflux pumps went up. Instead, the transcriptome sequencing (RNA-seq) data revealed a gene expression profile resembling that of a "stringent" RNA polymerase where protein and DNA biosynthesis pathways were downregulated but pathways to combat various stresses were upregulated. Some of these activated stress pathways are also controlled by the general stress sigma factor RpoS. The data presented here also show that compensatory mutations can act synergistically to further increase antibiotic resistance to a level similar to the efflux pump-proficient parental strain. Together, the findings highlight a remarkable genetic ability of bacteria to circumvent antibiotic assault, even in the absence of a major intrinsic antibiotic resistance mechanism.

IMPORTANCE Antibiotic resistance among bacterial pathogens is a chronic health concern. Bacteria possess or acquire various mechanisms of antibiotic resistance, and chief among them is the ability to accumulate beneficial mutations that often alter antibiotic targets. Here, we explored *E. coli*'s ability to amass mutations in a background devoid of a major constitutively expressed efflux pump and identified mutations in several regulatory genes that confer resistance by activating specific or pleiotropic mechanisms.

KEYWORDS antibiotic resistance, regulation of antibiotic resistance, stress regulon, efflux pumps

Efflux pumps (EPs) are one of the most ubiquitous and intrinsic means by which bacteria avoid killing by a wide spectrum of antibiotics. Although there are at least six major superfamilies of EPs present in Gram-negative bacteria (1), some of which, including the resistance-nodulation-division (RND) family of EPs, form a transenvelope complex to expel antibiotics directly from inside to outside the cell (2). One of the RND-type EPs, the tripartite complex of AcrAB-TolC proteins from *Escherichia coli*, represents the most exhaustively studied multidrug-resistant (MDR) efflux system (3). AcrB is the drug-proton antiporter, TolC is the outer membrane channel protein, and AcrA connects TolC and AcrB to complete the assembly of a functional EP (4). TolC is the common denominator of all known trans-envelope antibiotic EP complexes (2, 5, 6).

Citation Cho H, Misra R. 2021. Mutational activation of antibiotic-resistant mechanisms in the absence of major drug efflux systems of *Escherichia coli*. J Bacteriol 203:e00109-21. https://doi.org/10.1128/JB.00109-21.

Editor Laurie E. Comstock, Brigham and Women's Hospital/Harvard Medical School

Copyright © 2021 American Society for Microbiology. All Rights Reserved.

Address correspondence to Rajeev Misra, rajeev.misra@asu.edu.

Received 23 February 2021
Accepted 30 April 2021
Accepted manuscript posted online 10 May 2021
Published 22 June 2021

Although the *E. coli* genome codes for multiple drug efflux systems (7), only the AcrAB-TolC complex is constitutively expressed to confer a robust intrinsic drug resistance phenotype (8). Consequently, cells lacking any one component of the AcrAB-TolC tripartite complex display hypersusceptibility to a large number of antibiotics (5, 8, 9). Only when the AcrAB drug efflux system is genetically disabled can mutations (10–12) or multicopy plasmid clones (7, 13) be obtained that confer antibiotic resistance due to the upregulation of normally silent or weakly expressed EPs, such as AcrEF. The most frequent spontaneous genetic event that causes the activation of the AcrEF efflux pump is the acquisition of an insertion sequence (IS element) in the promoter region of the *acrEF* operon (10–12). Once activated, the AcrEF-TolC efflux system confers the same level of drug resistance as the constitutively expressed AcrAB-TolC system (12).

Both local and global regulators are known to modulate expression of the *acrAB* and *acrEF* genes. *acrR*, transcribed divergently from the *acrAB* genes, codes for a repressor of *acrAB* (14). Inactivation of *acrR* further increases *acrAB* expression and drug resistance (9, 10). AcrS, expressed from a gene located divergently from *acrEF*, also represses *acrAB* expression but not that of the adjacent *acrEF* genes (15). MarA, SoxS, and Rob are known to positively regulate *acrAB* expression in response to various environmental and chemical stimuli (16). In contrast to operon-specific regulators AcrR and AcrS, H-NS, a global transcription regulator (17), is known to repress expression of several EP genes, including *acrEF*, *acrD*, *mdtEF*, *macAB*, and *emrKY* (18). Genetic screening of a transposon library in the Δ*acrB* background revealed that inactivation of the *crp* gene, which codes for a global catabolite regulator, derepresses expression of the *mdtEF* genes (19). These examples demonstrate that mutations are the common means by which expression of normally dormant EP systems can be activated to partially or fully compensate for the loss of the major and constitutively expressed AcrAB drug efflux system. It is worth mentioning that, unlike the mutationally activated EPs mentioned above, the MdtABC drug efflux system was identified among plasmid clones expressing either the entire operon of *mdtABCD-baeSR* (13) or just the regulatory gene, *baeR* (13, 20).

Because of the slow pace by which new antibiotics are being discovered and the high clinical relevance of EPs in antibiotic resistance, inhibitors are being sought to block EP activity and thus increase the efficacy of existing drugs. The principal targets of EP inhibitors (EPIs) are the pump proteins that capture the substrate antibiotics before pumping them out (21–23). While research on EPIs is ongoing, their clinical application so far has been constrained due primarily to the toxic side effects on mammalian cells. Even if this constraint can be overcome, it is unlikely that an EPI will block all different types of pump proteins, thus paving the way for dormant EPs to be mutationally activated and substitute for the inhibited pump. Moreover, EPI-independent, target-specific mutations could potentially arise to circumvent the antibiotic action (24, 25). Finally, under antibiotic stress conditions, other types of mutations accumulate that either reduce the intake of antibiotics (26) or broadly influence bacterial physiology to slow antibiotic-mediated killing (27). Cells with such mutations can survive long enough to then accumulate additional mutations to gain a higher level of resistance. Therefore, a deeper understanding of the mutationally activated antibiotic resistance mechanisms will be critical for developing a comprehensive mitigation strategy to combat antibiotic resistance.

Due to the central role AcrB plays in drug efflux, it has been the model target for EPI investigation (28). While disabling AcrB chemically or genetically would render cells hypersusceptible to antibiotics, it would also render the opportunity for mutational activation of secondary mechanisms of drug resistance (29). In this study, we tested this possibility by isolating antibiotic-resistant mutants from an *E. coli* strain lacking AcrAB. Moreover, since we and others have already shown that the mutational activation of AcrEF is the prominent secondary means by which AcrB-disabled cells regain drug resistance (10–12), we also deleted *acrE* from the Δ*acrAB* strain background. The whole-genome sequence analysis of resistant mutants revealed single mutations in

TABLE 1 Antibiotic-resistant isolates form a Δ*acrAB* Δ*acrE* strain[a]

Antibiotic-resistant isolate(s) (culture no.)	MIC of Nov/Ery (μg/ml)	Efflux pump dependence	Gene affected in resistant mutants (allele)	Mutation (aa change)
WT	64–128/128	NA	NA	NA
Δ*acrAB* Δ*acrE*	1/2	NA	NA	NA
TolC$^-$	0.5/1.0	NA	NA	NA
1, 2 (1)	2/16	MdtEF	*hns*	IS*1*::224
3 (1)	ND	MdtEF	*hns*	IS*1*::193
4 (2)	ND	MdtEF	*hns*	T399C (F133S)
5 (3)	ND	MdtEF	*hns*	T90C (L30P)
6, 7 (3)	2/8	MdtEF	*hns*	IS*5*::268
8 (4)	ND	MdtEF	*hns*	IS*1*::141
9 (4)	16/4	MdtABC	*baeS* (*baeS51*)	C310T (R104C)
10 (4)	16/2	MdtABC	*baeS* (*baeS52*)	T104A (F35Y)
11 (4)	ND	MdtABC	*rpoB* (*rpoB53*)	G1361T (R454L)
12 (5)	2–4/8–16	MdtEF	likely *cyaA*	?
13 (5)	ND	MdtABC	*rpoB* (*rpoB55*)	T1295G (L432R)
14 (6)	ND	MdtABC	*rpoB* (*rpoB57*)	A443C (Q148P)
15 (6)	4/4–8	MdtABC	*rpoB* (*rpoB58*)	G1346T (G449V)
16 (6)	16/2	MdtABC	*baeS baeS59*	T895C (S299P)
17 (6)	32/4	MacAB	?	?
18 (7)	8–16/2	MdtABC	*baeS* (*baeS61*)	A76C (S26R)
19 (7)	2/8	MdtEF	*crp*	G41A (W14stop)
20 (7)	16/2	MdtABC	*baeS* (*baeS63*)	A1285G (N429D)

[a]ND, not determined; NA, not applicable; Nov, novobiocin; Ery, erythromycin; aa, amino acid; ?, mutation or affected gene is not revealed. Numbers after insertion sequence (IS) designation represent the *hns* nucleotide number at the insertion site.

four different regulatory genes. Here, we describe these mutants and the mechanisms by which they confer antibiotic resistance.

RESULTS AND DISCUSSION

Rationale and strategy for mutant isolation. One of our aims in this study was to identify mutations that restore antibiotic resistance in *E. coli* cells lacking the AcrAB EP, which has been the main target of EPI studies in *E. coli* (21, 28). When cells with a defective AcrAB EP system are challenged with antibiotics, resistant mutants frequently carry compensatory mutations that now activate the normally silent AcrEF EP (10–12). Because AcrAB and AcrEF share high sequence homologies, they are unsurprisingly inhibited by the same EPI (12). We therefore sought to identify secondary pathways of antibiotic resistance independent of AcrAB and AcrEF EPs. This was facilitated by simultaneously deleting the *acrAB* and *acrE* genes from our starting strain. Next, we wanted to avoid antibiotic target-specific mutations since, in almost all cases, targets of the commonly used antibiotics are already known. To achieve this, we simultaneously employed two different antibiotics, novobiocin and erythromycin, which target different cellular activities. Novobiocin inhibits DNA gyrase (B subunit) and topoisomerase IV (B subunit) enzymes, and resistant mutants carry alterations in their respective genes (30, 31). Erythromycin inhibits protein synthesis by targeting the 50S ribosomal subunit (32). Mutation-based resistance to erythromycin is gained by alterations in the 50S subunits proteins or 23S rRNA (33–35). Given that novobiocin and erythromycin affect unrelated cellular components and activities, their simultaneous use in our selection eliminated the possibility of isolating antibiotic target-specific mutations. Thus, the use of a Δ*acrAB* Δ*acrE* strain and two unrelated antibiotics in the selection of antibiotic-resistant mutants narrowed the scope of mutationally derived resistance pathways to those that either reduce drug intake, activate a dormant drug efflux system, or produce broad physiological changes.

Antibiotic-resistant mutants. In the AcrAB-positive (AcrAB$^+$) or AcrEF$^+$ strains, the MICs for novobiocin and erythromycin are around 64 to 128 μg/ml and 128 μg/ml, respectively; while in a Δ*acrAB* Δ*acrE* strain, the MICs for these antibiotics drop to between 1 and 2 μg/ml, respectively (Table 1). When both antibiotics are present in the medium, the MICs in AcrAB$^+$ and Δ*acrAB* Δ*acrE* strains are around 64 μg/ml and 0.5 μg/ml, respectively. To isolate antibiotic-resistant mutants, we chose the antibiotic

concentration of 2.5 μg/ml each of novobiocin and erythromycin or 5 times the combined MIC observed in the Δ*acrAB* Δ*acrE* strain. Roughly 4×10^8 cells from eight independently grown overnight cultures in lysogeny broth (LB) were plated on lysogeny broth agar (LBA) medium containing 2.5 μg/ml each of novobiocin and erythromycin. Plates were incubated for 48 h, although some resistant mutants arose after 24 h of incubation. The frequency of antibiotic-resistant mutants varied from 1×10^{-7} to 1×10^{-8}, indicating the presence of null and missense mutations in the revertants. Four resistant colonies from each of the eight independent cultures were purified on LBA containing 1.25 μg/ml of the two antibiotics since purification on the original antibiotic plates severely impaired growth of most revertants. Even on LBA containing the smaller amounts of the two antibiotics, only 20 out of 32 mutants derived from 7 independent cultures produced stable, homogenous colonies. These surviving 20 antibiotic-resistant mutants were further characterized.

Sorting of antibiotic-resistant mutants. We first conducted some simple phenotypic and genetic tests in an attempt to differentiate various mutants from each other. The removal of the *tolC* gene by P1 transduction of a null *tolC*::Tn*10* allele reversed the antibiotic resistance phenotype of all 20 mutants, indicating that their mechanism of resistance requires the presence of TolC, which is a common denominator of all known trans-envelope antibiotic EP complexes (2). We then systematically deleted the remaining TolC-dependent EP complex genes (one system at a time) from the resistant mutants to decipher the specific pathways. In 10 mutants, deletion of *mdtE* (of the MdtEF complex) reversed the antibiotic resistance phenotype, while in nine other mutants, deletion of *mdtA* (of the MdABC complex) did the same. In the last isolate, resistance was dependent on the MacAB pump. Interestingly, 2 of the 10 MdtEF-dependent mutants exhibited a small-colony phenotype even on a nonselective medium and conferred resistance to the lambda phage. The LamB protein, which serves as the cell surface receptor of the lambda phage (36), is a part of the *mal* regulon whose expression is positively controlled by an operon-specific regulator, MalT, and the global regulatory system of cAMP receptor protein (cAMP-CRP) (37). We found that deletion of the *crp* gene from the Δ*acrAB* Δ*acrE* strain produced the same small-colony and antibiotic-resistant phenotypes as the two spontaneous antibiotic-resistant mutants described above. Finally, we determined MICs of selected mutants against novobiocin and erythromycin (Table 1). The MIC values of the individual mutants were lower than the $AcrAB^+$ parental strain (Table 1), indicating that none of the mutations in these selected isolates fully compensate for the loss of two major drug EPs.

Whole-genome sequence analysis of antibiotic-resistant mutants. Our initial attempts to localize mutations on the chromosome using classical genetic approaches (Hfr conjugations and P1 transductions) and targeted DNA sequence analysis guided us to the location of only a few mutations. This prompted us to carry out the whole-genome sequence (WGS) analysis of selected mutants (isolate nos. 5, 8, 9, 11, and 15), followed by targeted DNA sequencing from the remaining isolates to determine whether they, too, carry mutations in genes already identified by the WGS analysis. The combination of these two approaches identified mutations responsible for the antibiotic-resistant phenotype in 18 of the 20 isolates (Table 1).

MdtEF-dependent isolates carry compensatory mutations in the *hns* and *crp* genes. In 8 of the 10 isolates where antibiotic resistance was dependent on MdtEF, mutations were found within the *hns* gene (Table 1), which codes for a histone-like nucleoid structuring protein that helps condense bacterial chromosome and regulate transcription (17). In 6 of the *hns* mutants, transposition of the IS*1* or IS*5* element disrupted the *hns* coding region at four different locations. We suspect that all six *hns* mutants with an IS transposition produce structurally and functionally defective H-NS proteins. In the remaining two, a single base substitution produced an L30P or F133S change in the protein sequence. Both of these missense mutations were previously identified as defective in transcription regulation and dimer or heteromer (with StpA) formation (38, 39). As noted in the introduction, Nishino and Yamaguchi (18) showed that Δ*hns*-mediated antibiotic resistance phenotype is due to derepression of *acrEF*

and *mdtEF* operons. Since our starting strain was deleted for the *acrE* gene, the observed antibiotic resistance phenotype in these eight isolates is solely due to the derepression of *mdtEF* expression. Indeed, this conclusion is consistent with our data showing the MdtEF dependence of these eight mutants for antibiotic resistance. Notably, this is the first report of direct isolation of spontaneous *hns* mutants with compensatory mutations to overcome the loss of AcrAB and AcrEF EPs. To confirm that the loss of H-NS activity is responsible for the observed drug-resistant phenotype of the Δ*acrABE* strain, we transduced a Δ*hns*::Km^r allele into a fresh parental (Δ*acrABE*) background. The resulting Δ*acrABE* Δ*hns*::Km^r strain grew on LBA plates containing novobiocin and erythromycin (1.25 μg/ml of each), while the Δ*acrABE* strain expectedly grew poorly (see Fig. S1 in the supplemental material).

The two remaining MdtEF-dependent antibiotic-resistant mutants with a small-colony phenotype were found to be resistant to the lambda phage. Based on these phenotypes and the existing knowledge of the negative effect of cAMP-CRP on *mdtEF* expression (19), we directly sequenced the *crp* gene. In one isolate, we identified a missense mutation resulting in the replacement of the tryptophan codon 41 to a stop codon (Table 1). The second isolate did not carry a mutation in the *crp* gene; however, based on its phenotypic similarities to the *crp* mutant, we surmise that the mutation in this isolate possibly resides in the *cyaA* gene, which codes for the adenylate cyclase enzyme responsible for cAMP synthesis.

MdtABC-dependent isolates with compensatory mutations in the *baeS* gene. MdtABC represents a unique EP system because it contains two pump/substrate-binding proteins, MdtB and MdtC, which form a heteromer during the assembly of the complex (40, 41). MdtD, produced from the fourth gene of the *mdt* operon, plays no direct role in drug efflux (see below). The last two genes of the *mdt* operon, *baeSR*, code for the sensor kinase and response regulator, respectively, and positively regulate the expression of the *mdtABCD-baeSR* operon (13, 20, 42).

In 5 of the 9 MdtABC-dependent antibiotic-resistant mutants, direct DNA sequencing of the promoter region of the *mdtABCD-baeSR* operon and the *baeS* gene identified missense mutations only in the *baeS* gene (Table 1). When mutant *baeS* alleles were genetically replaced by the wild-type (WT) *baeS* allele using a highly linked *asmA*::Km^r marker, all mutants lost the resistant phenotype at an expected frequency (90%), thus indicating that mutations in the *baeS* gene are likely responsible for the antibiotic-resistant phenotype in these five isolates. One of the *baeS* alleles, *baeS51*, was transduced back into the clean parental strain background (Δ*acrABE*) using the linked *asmA*::Km^r marker. The mutant *baeS* allele cotransduced into the fresh background at an expected frequency of 90%, i.e., 11 out of 12 Km^r transductants tested displayed the novobiocin-resistant phenotype similar to the original *baeS51* isolate. These data thus further supported the notion that mutations in *baeS* are solely responsible for the antibiotic resistance phenotype. All five *baeS* mutations are unique and introduce a single amino acid substitution in the BaeS protein (Table 1). Given the positive regulatory role of *baeS* on the *mdtABCD-baeSR* operon, we theorize that the five novel *baeS* alleles isolated here alter the BaeS structure to constitutively elevate its kinase activity and/or reduce its phosphatase activity. This will cause persistent phosphorylation of BaeR, which, in turn, will bind to the *mdtABCD-baeSR* promoter region to increase expression of the operon. Although the true physiological signal(s) that activates *mdtABCD-baeSR* expression is not known, various studies have implicated indole (43), metals (44–47), flavonoids (46), and ethanol (48) as possible activating signals. Because these presumed signals broadly affect cell physiology and activate multiple stress-responsive regulatory pathways, it is difficult to separate the BaeSR-specific regulon from other stress regulons. Therefore, we used the constitutive *baeS* alleles isolated here to reveal the members of the BaeSR regulon and to show that the mutant *baeS* alleles indeed activate the MdtABC EP genes to confer the antibiotic-resistant phenotype.

Aside from *mdtABCD-baeSR*, the activated BaeSR system is known to positively regulate expression of *spy* (42) and *acrD* (49). Therefore, we employed a chromosomally

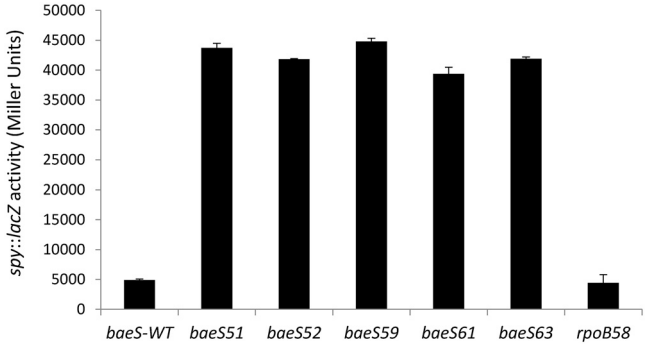

FIG 1 Effects of *baeS* and *rpoB58* mutations on *spy*::*lacZ* expression. β-Galactosidase assays were carried out from three independent cultures in duplicate. Error bars indicate standard deviations.

integrated *spy*::*lacZ* transcription fusion construct (50) to assess the expression status of the BaeSR regulon in our *baeS* mutant backgrounds. In all five *baeS* mutants, *spy*::*lacZ* expression was significantly upregulated ($>$8-fold) compared to the parental strain (Fig. 1), thus supporting the notion that these mutants activated the BaeSR regulon. Since all five *baeS* mutants showed a similar increase in *spy* expression, we used a representative mutant *baeS* allele, *baeS51*, to conduct transcriptome sequencing (RNA-seq) analysis. The RNA-seq data from *baeS51* and its parental strain were compared to generate the differential gene expression (DGE) profile.

Considering a $\log_2$ fold difference of $\geq$1.5 (or a $>$2.8 fold change in the linear scale) as a significant change in DGE, with *P* and false-discovery rate (FDR) values 0.01 and 0.05, respectively, we found that expression of 38 genes in the *baes51* mutant was upregulated, while that of 34 genes was downregulated (for a complete list of genes, see Table S1). The most highly upregulated genes included *spy* and *mdtABCD-baeSR* (Table 2), thus validating our hypothesis that the MdtABC-dependent antibiotic-resistant phenotype of the *baeS* mutant is due to increased expression of the *mdtABC* efflux genes. The observed elevated expression of the *spy* gene in the RNA-seq data (Table 2) is consistent with the *spy*::*lacZ* fusion data (Fig. 1).

Expression of *acrD* and, interestingly, that of many genes of the iron regulon was also upregulated (Table 2). Previous gene expression studies identified *acrD* as a part of the BaeSR regulon (43, 49), although a recent study suggested an indirect regulation of *acrD* by BaeSR (51). AcrD is an "orphan" drug EP protein that requires AcrA (of the AcrAB EP) to assemble into a functional drug efflux complex (52). Since our starting strain was Δ*acrAB*, it is unlikely that increased expression of *acrD* alone would confer drug resistance in the *baeS51* mutant. Nevertheless, to confirm that the observed antibiotic-resistant phenotype of the *baeS51* mutant is solely due to elevated expression of the *mdtABC* EP, we constructed an in-frame deletion of the *mdtA* gene in the *baeS51* background using the lambda Red-mediated recombination method (53). The in-frame deletion of *mdtA* reversed the antibiotic-resistant phenotype of the *baeS51* mutant (Fig. S2), thus confirming that enhanced expression of MdtABC EP is the sole cause of the observed antibiotic resistance.

As noted above, expression of *mdtD*, the fourth gene of the *mdtABCD-baeSR* operon, was also significantly upregulated (Table 2). Although MdtD is not a drug EP (7), it was shown to be a proton-dependent transporter of the major facilitator superfamily that exports iron citrate, hence the alternate name IceT (54). These authors also found that cells overexpressing MdtD have reduced levels of free intracellular iron. Consequently, a dramatic increase in *mdtD* (*iceT*) expression in the *baeS51* mutant would likely cause depletion of free intracellular iron. If so, this would cause an increased expression of genes involved in iron acquisition, which is supported by the findings of our DGE analysis (Table 2 and Table S1). We also noted elevated expression of genes of the *psp* operon (Table 2), which is involved in repairing proton leakage due

TABLE 2 Activation of the BaeSR regulon by the constitutionally active *baeS51* allele[a]

	baeS51			*rpoB58*		
Gene	**Log_2 FC**	***P* value**	**FDR**	**Log_2 FC**	***P* value**	**FDR**
BaeSR regulon genes						
spy	8.11	7.20E−27	3.35E−23	(0.37)	(0.04)	(0.09)
mdtA(*BCD-baeSR*)	5.22	3.78E−24	4.4E−21	(0.12)	(0.42)	(0.59)
mdtB	4.74	1.87E−24	2.9E−21	(0.12)	(0.56)	(0.71)
mdtC	4.89	5.84E−26	1.36E−22	(0.14)	(0.41)	(0.58)
mdtD	4.49	4.70E−20	3.13E−17	(0.25)	(0.17)	(0.31)
baeS	4.18	1.84E−22	1.72E−19	(0.27)	(0.17)	(0.31)
baeR	(1.33)	1.33E−13	1.82E−11	(0.19)	(0.07)	(0.16)
acrD	2.53	3.77E−22	2.92E−19	(−0.08)	(0.61)	(0.75)
tolC	(0.60)	6.45E−09	2.29E−07	(−0.11)	(0.53)	(0.68)
tnaC(*AB*)	(−1.30)	0.009	0.035	(0.02)	(0.95)	(1.00)
tnaA	(−1.22)	6.73E−11	4.54E−09	(0.17)	(0.45)	(0.62)
tnaB	(−1.34)	2.01E−11	1.46E−09	(0.43)	(0.22)	(0.38)
Iron regulon genes						
entC(*EBAH*)	3.55	1.56E−13	2.02E−11	(−1.12)	0.004	0.02
entE	2.92	3.20E−12	2.92E−10	(−0.98)	0.004	0.02
entB	3.73	4.03E−14	7.49E−12	(−0.52)	(0.10)	(0.21)
entA	2.19	3.94E−14	7.49E−12	(−0.33)	(0.15)	(0.28)
entH	3.09	8.66E−14	1.34E−11	(−0.002)	(0.99)	(1.00)
fes(*ybdZ-entF-fepE*)	(1.24)	0.0002	0.0014	(0.08)	(0.85)	(0.94)
ybdZ	2.97	0.008	0.033	(−0.59)	(0.34)	(0.51)
entF	2.39	1.54E−14	3.58E−12	(−0.20)	(0.26)	(0.43)
fepE	(0.005)	(0.99)	(1.00)	(−0.24)	(0.39)	(0.56)
yncE	2.96	1.60E−16	6.21E−14	(−0.37)	(0.22)	(0.38)
fepA	2.83	2.20E−16	7.33E−14	(−0.12)	(0.63)	(0.77)
cirA	2.12	6.65E−14	1.11E−11	(0.26)	(0.16)	(0.30)
fepC	2.11	3.26E−07	6.17E−06	(0.22)	(0.51)	(0.67)
yqjH	1.98	3.83E−12	3.3E−10	(−0.14)	(0.56)	(0.71)
fhuF	1.82	3.37E−12	2.96E−10	(−0.03)	(0.93)	(0.99)
entS	1.48	3.86E−05	0.0004	(−0.06)	(0.86)	(0.95)
PSP operon genes						
pspA(*BCDE*)	2.13	1.91E−16	6.8E−14	(0.34)	(0.02)	(0.06)
pspB	1.95	3.06E−09	1.21E−07	(0.13)	(0.52)	(0.68)
pspC	1.68	4.38E−12	3.64E−10	(0.11)	(0.54)	(0.69)
pspD	1.79	5.74E−07	1E−05	(0.12)	(0.61)	(0.76)
pspE	(−0.45)	9.22E−06	0.00011	(1.34)	4.64E−06	0.0002
pspG	1.92	7.54E−08	1.77E−06	(−0.29)	(0.29)	(0.46)
pspF	(−0.35)	0.0005	0.003	(−0.11)	(0.54)	(0.69)

[a]Genes of an operon are shown in parentheses after the first gene. Number in parentheses reflect below-the-cutoff values of ≥1.5 (log_2 FC), ≤0.01 (*P*), and ≤0.05 (FDR).

to membrane damage (55). It is possible that overexpression of MdtABC and MdtD, the two proton-dependent transporters, partially disrupts the proton gradient across the membrane, thus elevating the expression of the *psp* operon in the *baeS51* mutant.

MdtABC-dependent isolates with compensatory mutations in the *rpoB* gene. In 4 of the 9 MdtABC-dependent antibiotic-resistant mutants, WGS analysis identified four different missense mutations in the *rpoB* gene, which codes for the beta subunit of the RNA polymerase (RNAP). Replacement of the mutant *rpoB* alleles by wild type via P1 transduction of a linked Tc^r (*btuB*::Tn*10*; >80% linked to *rpoB*) marker reversed the antibiotic resistance phenotype, thus indicating that the *rpoB* mutations are likely responsible for the resistance phenotype in these isolates. Using the linked *btuB*::Tn*10* marker, all four *rpoB* alleles were reintroduced by P1 transduction into the fresh parent strain background (Δ*acrABE*). In all cases, mutant *rpoB* alleles conferring the novobiocin-resistant phenotype cotransduced with *btuB*::Tn*10* at an expected frequency of around 80%, thus further supporting the conclusion that mutations in *rpoB* are solely responsible for the antibiotic-resistant phenotype. RNAP has been a well-known target

TABLE 3 *rpoB58*-affected genes involved in protein synthesis[a]

Gene	Log_2 FC	*P* value	FDR	Function
rluB	−1.94	2.06E−06	0.0001	23S rRNA pseudouridine synthase
sspB	−1.59	5.60E−08	1.00E−05	Stringent starvation protein B
rlmN	−1.57	3.11E−06	0.0001	23S rRNA methyltransferase
rplK(*rplAJL-rpoBC*)	−1.57	4.41E−06	0.0002	L11 protein of 50S
rplA	−1.45	7.23E−05	0.001	L1 protein of 50S
rplJ	−1.10	0.0001	0.002	L10 subunit of 50S
rplL	−1.07	0.0003	0.003	L7/L12 dimer protein of 50S
rpoB	(−0.55)	(0.06)	(0.14)	Beta subunit of RNAP
rpoC	(−0.39)	(0.05)	(0.13)	Beta-prime subunit of RNAP
suhB	−1.55	6.64E−06	0.0002	30S assembly
rpsT	−1.54	5.38E−07	4.47E−05	S20 protein of 30S
prfC	−1.47	0.001	0.01	Peptide chain release factor 3
yidD	−1.42	8.43E−05	0.001	Membrane protein insertion factor
tufB	−1.41	0.0002	0.002	Translation elongation factor Tu 2
rpsL(*rpsG-fusA-tufA*)	−1.27	7.37E−05	0.001	S12 protein of 30S
rpsG	−1.18	0.001	0.01	S7 protein of 30S
fusA	−1.06	0.001	0.01	Elongation factor G
tufA	(−0.54)	0.01	0.04	Translation elongation factor Tu 1
efp	−1.22	3.30E−06	0.0001	Protein elongation factor EF-P
rplU(*rpmA*)	−1.15	8.34E−06	0.0003	L21 protein of 50S
rpmA	−1.21	3.07E−05	0.001	L27 protein of 50S
rpmH(*rnpA*)	−1.18	5.63E−05	0.001	L34 protein of 50S
rnpA	−1.35	9.53E−06	0.0003	RNase P (tRNA processing)
rpsU	−1.17	2.76E−06	0.0001	S21 protein of 30S
rpsB	−1.17	0.0003	0.003	S2 protein of 30S
rlmG	−1.17	0.0004	0.004	Methyltransferase of 23S rRNA
yidC	−1.16	0.003	0.02	Membrane protein insertase
prmB	−1.15	0.002	0.01	50S methyltransferase
queA	−1.15	2.62E−05	0.001	*S*-Adenosylmethionine:tRNA ribosyltransferase-isomerase
rpsP(*rimM-trmD-rplS*)	−1.13	5.92E−05	0.001	S16 protein of 30S
rimM	−1.01	0.002	0.01	30S maturation factor
trmD	−1.00	0.004	0.02	tRNA methyltransferase
rplS	(−0.87)	0.006	0.03	L19 protein of 50S
rsmC	−1.07	1.63E−05	0.0004	16S rRNA methyltransferase
rpsF	−1.06	0.001	0.01	S6 protein of 30S
rpmE	−1.04	2.89E−05	0.001	L31 protein of 50S
rlmL	−1.04	0.001	0.01	23S rRNA methyltransferase

[a]Genes of an operon are shown in parentheses after the first gene. Numbers in parentheses reflect below the cutoff values of ≥1.0 (log_2 FC), ≤0.01 (*P*), and ≤0.05 (FDR).

of rifampin (56), and rifampin-resistant mutations in *rpoB* can be readily isolated (57, 58). Since novobiocin and erythromycin do not target RNAP, it is unlikely that *rpoB* mutations isolated here confer resistance to these two antibiotics by specifically altering the RNAP structure.

Because the *rpoB* mutants, like the *baeS* mutants, were MdtABC dependent, we suspected that their antibiotic-resistant phenotype is also due to activation of the BaeSR regulon. However, *spy*::*lacZ* data did not support this hypothesis (Fig. 1). We then consider a possibility that RNAP mutants specifically increase the activity of certain specific promoters, including that of the *mdt* operon, to increase *mdtABC* expression without necessarily increasing the expression of the whole BaeSR regulon, including *spy*. To test this possibility, we generated a DGE profile by comparing the RNA-seq data from one of the mutant *rpoB* alleles, *rpoB58*, to that of its parent strain (Tables 2 to 6). Surprisingly, expression of the entire BaeSR regulon, including that of *mdtABCDbaeSR*, *spy*, *acrD*, and indirectly affected genes of iron and *psp* regulons was unaltered in the *rpoB58* mutant (Table 2). Therefore, the antibiotic-resistant phenotype of *rpoB58* is not due to increased expression of *mdtABC*, as we had expected.

Instead, the data suggest that the antibiotic-resistant phenotype of our mutant is the result of a cumulative effect of the basal expression of the *mdt* operon and pathways affected by *rpoB58* mutation. In the parental strain lacking the main EPs AcrAB and AcrEF, weakly expressed EPs, including MdtABC and MdtEF, presumably provide

TABLE 4 *rpoB58*-affected genes involved in tRNA and amino acid synthesis[a]

Gene	Log_2 FC	*P* value	FDR	Function
tRNA genes				
argX(*hisR-leuT-proM*)	−4.09	0.001	0.01	Arginine (GCC) tRNA
hisR	−1.82	0.001	0.01	Histidine (GUG) tRNA
leuT	ND	NA	NA	Leucine (CAG) tRNA
proM	−2.96	0.001	0.01	Proline (UGG) tRNA
leuU(*secG*)	−2.42	0.002	0.01	Leucine (GAG) tRNA
secG	−1.75	0.0004	0.003	Sec translocon subunit
glyW(*cysT-leuZ*)	ND	NA	NA	Glycine (GCC) tRNA
cysT	−2.30	0.01	0.02	Cystine (GCA) tRNA
leuZ	−1.97	0.0004	0.003	Leucine (UAA) tRNA
thrU(*tyrU-glyT-thrT-tufB*)	−2.26	0.002	0.01	Threonine (UGU) tRNA
tyrU	−1.48	0.001	0.004	Tyrosine (GUA) tRNA
glyT	−1.96	0.01	0.031	Glycine (UCC) tRNA
tufB	−1.41	0.0002	0.002	Translation elongation factor Tu 2
leuP	−2.21	0.0004	0.004	Leucine (CAG) tRNA
serV	−1.86	0.001	0.004	Serine (GCU) tRNA
leuW	−1.83	0.01	0.022	Leucine (UAG) tRNA
Amino acid genes				
metE	3.07	1.73E−11	2.68E−08	Methionine synthesis
lysC	2.41	0.002	0.01	Homoserine synthesis
hisG(*DCBHAFI*)	1.90	6.63E−08	1.10E−05	Histidine synthesis
hisD	1.85	3.12E−07	3.30E−05	Histidine synthesis
hisC	1.88	6.46E−07	4.93E−05	Histidine synthesis
hisB	1.49	1.34E−06	8.19E−05	Histidine synthesis
hisH	1.33	1.12E−05	0.0003	Histidine synthesis
hisA	1.34	2.02E−05	0.0005	Histidine synthesis
hisF	1.29	4.49E−06	0.0001	Histidine synthesis
hisI	1.26	4.44E−06	0.0002	Histidine synthesis
hisJ(*QMP*)	1.71	1.02E−06	6.89E−05	Histidine transport
hisQ	1.56	9.97E−06	0.0003	Histidine transport
hisM	1.41	8.05E−05	0.001	Histidine transport
hisP	1.23	0.002	0.010	Histidine transport
thrL(*ABCD*)	1.51	0.0002	0.002	Threonine synthesis
thrA	(0.76)	0.002	0.01	Threonine synthesis
thrB	(0.32)	(0.16)	(0.30)	Threonine synthesis
thrC	(0.35)	0.01	0.05	Threonine synthesis
thrD	ND	NA	NA	Threonine synthesis
leuL(*ABCD*)	1.17	(0.50)	(0.66)	Leucine synthesis (leader peptide)
leuA	1.29	2.55E−06	0.0001	Leucine synthesis
leuB	1.23	1.33E−05	0.0003	Leucine synthesis
leuC	1.34	7.29E−06	0.0002	Leucine synthesis
leuD	(0.88)	0.0002	0.002	Leucine synthesis
argI	1.21	0.0004	0.004	Arginine synthesis
ilvH	1.07	5.36E−05	0.001	Isoleucine synthesis
metC	1.04	4.00E−06	0.0002	Methionine synthesis

[a]Genes of an operon are shown in parentheses after the first gene. Numbers in parentheses reflect below the cutoff values of ≥1.0 (log_2 FC), ≤0.01 (*P*), and ≤0.05 (FDR). ND, not detected; NA, not applicable.

some basal level of resistance. We surmise this because when TolC, a common denominator of several EPs, is deleted from the parental strain, MICs for novobiocin and erythromycin further drop (Table 1). The MIC data show that resistance conferred by *rpoB58* is relatively modest (Table 1). The *rpoB58*-mediated resistance is MdtABC dependent because the removal of this EP lowers the resistance to a point where the *rpoB58* mutant alone fails the antibiotic screen test performed on a medium containing 1.25 μg/ml each of novobiocin and erythromycin. It is possible that individual mutations described here, including *rpoB58*, will increase cell survivability long enough to allow for the acquisition of additional mutations to further increase resistance and survival. We tested this by combining *rpoB58* and *baeS51* in one strain and observed an increase in novobiocin MIC from 4 μg/ml (*rpoB58*) and 16 μg/ml (*baeS51*) to 32 μg/ml in the

TABLE 5 *rpoB58*-affected genes involved in nucleic acid synthesis[a]

Gene	Log_2 FC	*P* value	FDR	Function
carA(B)	−2.88	2.98E−05	0.001	UMP biosynthesis
carB	−2.79	0.001	0.01	UMP biosynthesis
uraA	−2.32	0.0002	0.003	Uracil-H^+ symporter
pyrD	−1.96	5.19E−06	0.0002	Purine synthesis
upp	−1.92	3.24E−05	0.001	Pyrimidine salvage
purH(*purD*)	−1.86	0.0001	0.002	Purine synthesis
purD	−1.57	0.01	0.03	Purine synthesis
pyrL(*BI*)	−1.66	0.0001	0.002	Operon's leader peptide
pyrB	−1.24	0.0001	0.004	UMP synthesis
pyrI	−1.13	0.0013	0.01	UMP synthesis
guaC	−1.49	2.58E−05	0.001	Purine salvage
gpt	−1.49	1.54E−06	8.62E−05	Purine salvage
pyrC	−1.488	0.0004	0.003	Pyrimidine synthesis
guaB(*A*)	−1.44	0.002	0.013	Guanine synthesis
guaA	(−0.84)	(0.05)	(0.09)	GMP synthesis
cmk	−1.43	1.48E−07	1.91E−05	Pyrimidine salvage
purM(*N*)	−1.38	0.0002	0.002	Purine synthesis
purN	−1.39	0.003	0.02	Purine synthesis
cvpA(*purF-ubiX*)	−1.26	0.001	0.01	Colicin V production
purF	−1.36	0.01	0.03	Purine synthesis
ubiX	−1.03	0.0004	0.003	Prenylated $FMNH_2$ synthesis
holD	−1.29	0.0001	0.001	DNA Pol III subunit psi
purT	−1.26	0.001	0.01	Purine synthesis
pyrF(*yciH*)	−1.04	4.79E−05	0.001	UMP synthesis
yciH	−1.21	0.012	0.04	Putative translation factor
priB	−1.19	0.001	0.01	Primosomal replication protein
folA	−1.15	4.87E−06	0.0002	Dihydrofolate reductase
tdk	−1.15	0.002	0.01	Pyrimidine salvage
rapA	−1.12	0.001	0.004	RNAP recycling factor
rho	−1.08	1.31E−05	0.0003	Transcription termination
pyrE	−1.06	0.001	0.01	UMP synthesis
purL	−1.01	0.01	0.05	Purine synthesis

[a]Genes of an operon are shown in parentheses after the first gene. Numbers in parentheses reflect below the cutoff values of −1.0 or higher (log_2 FC), ≤0.01 (*P*), and ≤0.05 (FDR).

double mutant. Therefore, these compensatory mutations have the potential to restore a high level of antibiotic resistance by acting synergistically.

Mechanism of *rpoB58*-mediated antibiotic resistance. In an attempt to comprehend the mechanism of antibiotic resistance in the *rpoB58* mutant, we further analyzed the *rpoB58*/*rpoB*-WT DGE profile. Since RNAP transcribes all genes, the expression of many genes was significantly (log_2 fold change [FC] ≥ 1.5; $P \leq 0.01$; FDR ≤ 0.05) affected by the *rpoB58* mutation. Expression of 158 genes increased, while that of 58 genes decreased (a full list of affected genes is shown in Table S2). The expression of genes located further down in an operon is naturally lower than those present at the beginning and thus failed to meet the log_2 FC threshold of 1.5. Moreover, since many genes that are affected by *rpoB58* code for essential functions such as protein and DNA synthesis, their expression is unlikely to change significantly. Nevertheless, given that expression of a large number of genes was affected, it made it challenging to determine which ones are responsible for the resistant phenotype or eliminate the possibility of a pleiotropic effect. Therefore, we sought cues from published work to help narrow down the genes/operons whose increased or decreased expression could potentially account for the antibiotic resistance phenotype. Pietsch et al. (59) isolated *rpoB* mutations among ciprofloxacin-resistant isolates and reported a modest (2- to 4-fold) increase in the expression of MdtK EP. However, their *rpoB* mutations, which are different from those isolated in this study, arose only after the accumulation of mutations in other genes and had no impact alone on antibiotic resistance. In contrast, *rpoB58* is the sole cause of antibiotic resistance without altering *mdtK* expression (log_2

TABLE 6 *rpoB58*-affected genes involved in osmotic, oxidative, and acid stresses[a]

Gene	Log_2 FC	*P* value	FDR	Function
Osmotic stress genes				
osmE	2.18	1.16E−06	7.70E−05	Osmotically induced lipoprotein
treA	2.11	8.29E−07	5.85E−05	Periplasmic trehalase
osmY	1.73	3.47E−06	0.0001	Periplasmic chaperone
otsB(*A*)	1.60	6.80E−05	0.001	Trehalase-6-P phosphatase
otsA	1.35	6.02E−06	0.0002	Trehalase-6-P synthase
osmF(*yehYX*)	1.53	5.38E−06	0.0002	Glycine betaine transporter
yehY	1.34	6.28E−05	0.001	Glycine betaine transporter
yehX	1.21	4.18E−05	0.001	Glycine betaine transporter
yehW	(0.35)	(0.12)	(0.24)	Glycine betaine transporter
osmB	1.29	0.0003	0.003	Osmotically induced lipoprotein
Oxidative stress genes				
hmp	2.78	2.13E−07	2.54E−05	Nitric oxide dioxygenase
ytfE	2.24	0.0001	0.001	Fe-S cluster repair protein
sufA(*BCDSE*)	2.12	0.0003	0.003	Fe-S cluster assembly protein
sufB	1.97	0.0003	0.003	Fe-S cluster scaffold complex
sufC	1.78	0.0001	0.001	Fe-S cluster scaffold complex
sufD	1.82	7.68E−06	0.0002	Fe-S cluster scaffold complex
sufS	1.39	5.54E−06	0.0002	L-cysteine desulfurase
sufE	1.36	2.65E−05	0.001	Sulfur carrier protein
yodD	2.05	0.0001	0.002	Stress (H_2O_2)-induced protein
wrbA	1.87	2.19E−05	0.001	NAD(P)H:quinone oxidoreductase
osmC	1.69	1.16E−05	0.0003	Osmo-inducible peroxiredoxin
katE	1.61	6.87E−06	0.0002	Catalase II (hydroperoxidase II)
bfr	1.42	7.07E−06	0.0002	Betrioferritin
dps	1.42	0.0001	0.001	Iron-sequestering nucleoprotein
acnA	1.41	1.32E−06	8.16E−05	Aconitase hydratase A
grxB	1.20	4.89E−07	4.21E−05	Reduced glutaredoxin 2
Acid tolerance genes				
ycgZ(*ymgA-ariR-ymgC*)	2.61	1.55E−07	1.95E−05	Transcription regulator
ymgA	3.30	7.82E−08	1.22E−05	Regulator of acid resistance
ariR	3.98	5.42E−08	1.00E−05	Regulator of acid resistance
ymgC	3.86	6.22E−07	4.89E−05	Regulator of acid resistance
asr	1.91	1.74E−05	0.0004	Acid shock protein
slp(*dctR*)	1.68	0.0003	0.003	Starvation lipoprotein
dctR	1.42	0.01	0.05	Transcription regulator
ybaS(*T*)	1.88	0.002	0.013	Glutaminase I
ybaT	1.05	0.004	0.02	Putative transporter
gadE	1.82	0.0002	0.002	Acid-responsive regulator of *gadBC*
gdhA	1.51	1.31E−07	1.79E−05	Glutamate dehydrogenase
rpoS	1.39	2.18E−06	0.0001	Sigma S factor
gadB(*C*)	1.11	0.002	0.01	Glutamate decarboxylase B
gadC	(0.74)	0.003	0.025	L-Glu:4-aminobutyrate transporter

[a]Genes of an operon are shown in parentheses after the first gene. Numbers in parentheses reflect below the cutoff values of ≥1.0 (log_2 FC), ≤0.01 (*P*), and ≤0.05 (FDR).

FC of −0.05). The fact that expression did not increase for any known EPs (AcrD, CusCFA, EmrAB, EmrKY, MacAB, MdtABC, and MdtEF) in the *rpoB58* mutant (Table 2 and Table S2), which already lacks AcrAB and AcrEF, indicated that a pleiotropic mechanism is likely responsible for the antibiotic-resistant phenotype.

RpoB58 transforms RNAP into a "stringent" polymerase. When analyzing the larger DGE data, we subsequently noted that expression of many genes involved in protein (Tables 3 and 4) and nucleic acid (Table 5) synthesis was downregulated, while expression of genes involved in amino acid synthesis was upregulated (Table 4). (Note that we lowered the log_2 FC threshold to ±1.0 since many affected genes encode essential functions and their expression is not expected to change too drastically). The observed pattern of gene expression in *rpoB58* is strikingly reminiscent of that seen during stringent response (SR) (60), which is classically triggered under amino acid

starvation conditions (61). A hallmark of SR is the increased synthesis of an alarmone, (p)ppGpp (61, 62), which binds to RNAP and modulates its activity (63). Additionally, we noted increased expression of genes involved in various stress pathways, including osmotic stress, oxidative damage, and acid tolerance (Table 6). Most of these genes are regulated by RpoS sigma factor, which is best known for its role in controlling gene expression during entry into the stationary growth phase (64, 65). Expression of some of these stress pathway genes is also regulated by (p)ppGpp. Interestingly, both SR and RpoS have been implicated in conferring a low level of resistance or tolerance to antibiotics (66); for a recent review on SR's role in antibiotic resistance, see reference 67. The exact mechanism by which SR and RpoS contribute to antibiotic resistance is not clear, but it is likely to involve pleiotropic changes in bacterial physiology, ranging from retarded growth due to altered metabolism and macromolecular synthesis to elevated expression of stress-reducing enzymes (68). Based on this, we postulate that pathways affected by the SR/RpoS regulatory systems are in part responsible for the *rpoB58* phenotype.

Experimental verification that the RNAP mutant has adapted a stringent state. The close resemblance of the DGE profile of the *rpoB58* mutant to that normally seen during SR induction (60) strongly suggests that the mutant RNAP has assumed a stringent state even under normal (nonstarved) growth conditions. There have been reports of RNAP mutants with mutations in *rpoB* or *rpoC* (coding for the beta-prime subunit of RNAP) that behave like stringent RNAP. For example, transcription studies by Zhou and Jin (69) found that certain RNAP mutants, with altered RpoB subunits, behaved like stringent polymerase even without SR-inducing conditions. During SR, (p)ppGpp binds to two distinct sites on RNAP to alter its activity and transcription from selected promoters (for a recent review, see reference 70). Binding of (p)ppGpp to one of the sites on RNAP is facilitated by a small protein, DksA (63, 71). Cells lacking DksA behave similarly, but not identically, to those unable to synthesize (p)ppGpp (72, 73). One of the well-established phenotypes of "relaxed" mutants lacking (p)ppGpp or DksA is their inability to grow on minimal medium not supplemented with certain amino acids (72). Without bound (p)ppGpp or DksA, WT RNAP is unable to properly transcribe from promoters of certain amino acid operons (74). Indeed, mutations in *rpoB* or *rpoC* were isolated as suppressors of this defective growth phenotype of Δ*dksA* on a minimal medium (75).

Based on these observations, we hypothesized that if the four *rpoB* mutants isolated here transform RNAP into a stringent state, as the DGE data already suggest for *rpoB58*, then these mutants may overcome Δ*dksA*-mediated amino acid auxotrophy. To test this, we transduced the Δ*dksA*::Km^r allele into strains expressing WT *rpoB* and the four mutant *rpoB* alleles. The strains from the rich medium were then purified on glycerol minimal medium not supplemented with amino acids. As can be seen in Fig. 2, Δ*dksA*::Km^r cells expressing WT *rpoB* were unable to grow on the glycerol minimal medium, even after 48 h of incubation at 37°C. However, all four *rpoB* mutants lacking DksA were able to grow, thus supporting the hypothesis that the four mutant RNAPs have adapted a stringent state. Interestingly, one of our *rpoB* mutants (*rpoB53* with an R454L substitution) was also isolated in the previously mentioned Δ*dksA* suppressor analysis (75). Another established phenotype of the stringent RNAP is reduced expression of the rRNA operon. However, since ribosomal RNAs were removed prior to the RNA-seq analysis, we could not determine the status of the rRNA operon in the *rpoB58* mutant. Therefore, we employed an *rrnB*-P1::*lacZ* fusion to determine the effect of *rpoB58* on rRNA operon transcription. The *rpoB58* mutation reduced *rrnB*-P1::*lacZ* expression by 40% but had no effect on the activity of a control *lacUV5*::*lacZ* construct (Fig. 3). These results are consistent with our hypothesis that the mutant RNAP has adapted a stringent state.

DksA dependence on mutant RNAP-mediated antibiotic resistance. Although the *rpoB58* mutation bypasses the need for DksA for growth on minimal medium, it is unclear whether it can also bypass DksA's requirement for antibiotic resistance. A recent study showed increased susceptibility of an *E. coli* strain lacking *dksA* to 12

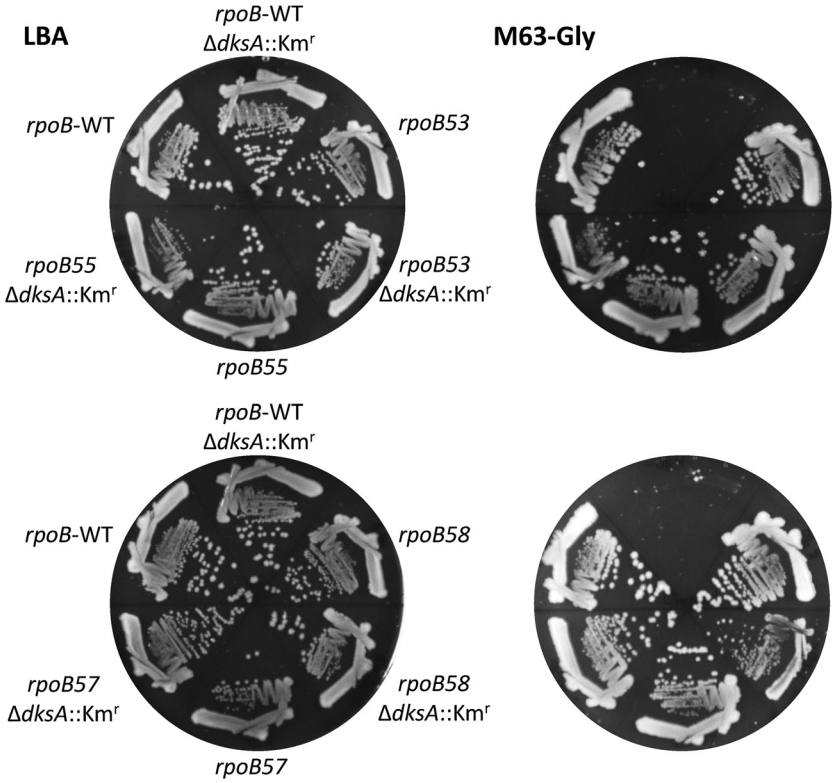

FIG 2 Effect of Δ*dksA* on the ability of strains expressing wild-type (WT) or mutant alleles of *rpoB* to grow on M63 salt-based minimal medium. Strains were first grown on the rich medium (LBA) for 24 h (left two plates). Individual colonies from LBA were then streaked on M63 minimal medium supplemented with glycerol (M63-Gly) and grown at 37°C for 48 h (right two plates). Key genetic characteristics are shown.

different antibiotics (76), thus indicating a role for DksA in maintaining intrinsic antibiotic resistance. We first verified the effect of Δ*dksA* in an AcrAB$^+$ background expressing WT or RpoB58 RNAP and noted a 2- to 4-fold (from 64 to 128 μg/ml to 32 μg/ml) reduction in the novobiocin MIC (Table S3). We then compared novobiocin MIC values of *rpoB58* and *rpoB58* Δ*dksA* without AcrAB and AcrEF to see whether DksA is required for *rpoB58*-mediated antibiotic resistance in a background lacking two major EPs. Deletion of *dksA* from the *rpoB58* background lowered the MIC for novobiocin from 4.0 μg/ml to $\leq$1.0 μg/ml, thus showing that *rpoB58*-mediated antibiotic resistance depends on DksA (Table S3). Unlike Δ*dksA*, Δ*rpoS* had no effect on novobiocin MIC, either in the WT or the efflux-defective parental (Δ*acrABE*) background (Table S3).

Conclusions and perspectives. Although EPIs can potentiate antibiotic efficacy, it is unknown whether bacteria can overcome a combined EPI and antibiotic regimen by

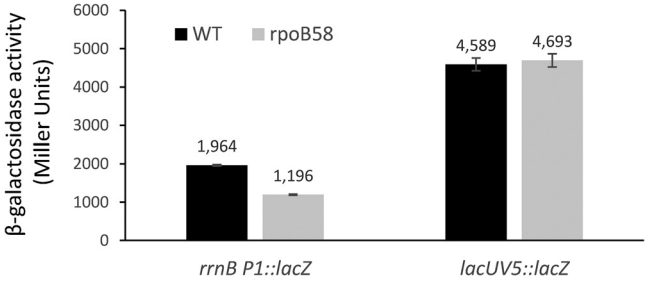

FIG 3 Effect of *rpoB58* mutation on *rrnB* P1::*lacZ* and *lacUV5*::*lacZ* expression. β-Galactosidase assays were carried out from three independent cultures in duplicate. Error bars indicate standard deviations.

accumulating mutations. We tested this possibility by analyzing antibiotic-resistant mutants from cells lacking the two major antibiotic EPs, AcrAB and AcrEF, which we considered equivalent to complete inhibition of these pumps by an EPI. The genetic makeup of the starting strain (Δ*acrAB* Δ*acrE*) and the simultaneous use of mechanistically unrelated antibiotics, novobiocin and erythromycin, eliminated target-specific mutations and instead enriched for those that either reduce drug intake, activate a dormant drug efflux system, or produce broad physiological changes. Mutations falling in the latter two categories were obtained, but not those that directly reduce drug intake.

Of the 20 antibiotic-resistant mutations isolated from the Δ*acrAB* Δ*acrE* background, 18 mapped in four regulatory genes, *baeS*, *crp*, *hns*, and *rpoB*. Of these, mutations in *baeS* conferred antibiotic resistance by activating expression of MdtABC. Antibiotic resistance resulting from *hns* and *crp* mutations could be mechanistically linked to the derepression of a single-drug EP system, MdtEF. In spite of the dependence of *rpoB* mutations on MdtABC for resistance, expression of *mdtABC* and genes coding for other known drug EPs did not go up, thus indicating a pleiotropic mechanism of resistance. DGE data from the *rpoB58* mutant showed that expression of many genes was affected. In particular, expression of genes involved in various stress pathways was impacted, including stringent (ppGpp; RelA/SpoT) and general stress (RpoS) responses, which have been implicated in conferring intrinsic antibiotic tolerance (66, 68, 77). Normally, these pathways are activated under certain stressful growth conditions (78), but by altering the gene expression profile, *rpoB58* transformed cells into a "stressed state," even under nonstressful growth conditions. Given the pleiotropic nature of *rpoB58*, it is difficult to pinpoint which specific pathway or combination of pathways is responsible for the antibiotic resistance phenotype. Nevertheless, it is clear that under *in vivo* growth conditions, pleotropic mechanisms likely play a crucial role in defending bacteria against various stressors, including antibiotics.

MATERIALS AND METHODS

Bacterial strains, genetic methods, and antibiotic susceptibility assays. Most bacterial strains used here are derived from RAM1292 (MC4100 Δ*ara714*, referred to as wild type [WT] [79]) and are listed in Table 7. Lysogenic broth (LB) was prepared from Difco LB EZMix powder. LB agar (LBA) was prepared using LB plus 1.5% agar (Becton Dickinson). When needed, kanamycin (25 μg/ml) and tetracycline (12.5 μg/ml) were added to LBA. Unless specified, all cultures were incubated at 37°C from 18 to 24 h. Bacteriophage P1-mediated transductions, using antibiotic resistance markers, were carried out as described previously (80). Antibiotic susceptibility was assessed by determining MICs of novobiocin and erythromycin by the 2-fold serial dilution method using 96-well microtiter plates. Approximately 10^5 cells were seeded in each well and grown for 18 h with gentle aeration in 200 μl LB supplemented with various concentrations of antibiotics. Optical density at 600 nm (OD_{600}) was read by VersaMax microplate reader. The MIC was determined to be the lowest antibiotic concentration that corresponded to OD_{600} of $<$0.1. All MIC experiments were carried out with three or more biological replicates.

***β*-Galactosidase assays.** These assays were carried out to measure gene expression and determine leakage of the cytoplasmic contents in the culture supernatant. β-Galactosidase activities were measured from three to six independent cultures in duplicate by the method described by Miller (81).

DNA sequence analysis. The whole-genome sequence analysis was carried out to determine the location of suppressor mutations. Bacterial chromosome was isolated using DNeasy blood and tissue kit from Qiagen and subjected to sequencing by Illumina's MiSeq system. Whole-genome sequencing reads for each sample were quality checked using FastQC v0.10.1 and aligned *Escherichia coli* K-12 MC4100 genome from the NCBI database (GenBank Assembly accession no. GCF_000499485.1) using Burrows-Wheeler short-read alignment tool, BWA version 0.7.15. After alignment, single nucleotide polymorphisms (SNPs) and indels were discovered following GATK Best Practices workflow of Germline short variant discovery (https://gatk.broadinstitute.org/hc/en-us/articles/360035535932-Germline-short-variant-discovery-SNPs-Indels). Raw mapped reads were preprocessed by adding read groups, indexing, marking duplicates, sorting, and recalibrating base quality scores. Then variants were called by HaplotypeCaller. Per-base genome coverage was computed by bedtools genomecov. All regions with zero coverage were reported. Structural variations were identified by BreakDancer and LUMPY 0.2.13. The presence of nonsynonymous mutations was confirmed by Sanger sequencing using PCR-amplified fragments of the targeted region.

RNA-seq analysis. RNA was prepared from three to five independent cultures grown to mid-log phase, using the RNeasy minikit from Qiagen. Total RNA was ribo-depleted using Illumina's Ribo-Zero rRNA removal kit (bacteria) (Illumina catalog no. MRZB12424). The ribo-depleted RNA was then enzymatically sheared to roughly 150 bp using Kapa's HyperPrep RNA-seq kit (Roche; Kapa code KK8540). Kapa's HyperPrep RNA-seq, kit along with Illumina-compatible adapters (IDT no. 00989130v2), was also used for the remaining library construction. Separate libraries were constructed and sequenced from

TABLE 7 Bacterial strains used in this study

Strain	Characteristics	Reference no. or source
RAM1292	MC4100 Δ*ara714*	79
RAM2370	RAM1292 Δ*acrAB*::scar	12
RAM3027	RAM1292 *btuB*::Tn*10*	This study
RAM3028	RAM1292 *btuB*::Tn*10 rpoB58*	This study
RAM3133	RLG4996 (*lacZ-lacY-rrnB* P1::*lacZ*)	74
RAM3134	RLG4998 (*lacZ-lacY-lacUV5*::*lacZ*)	83
RAM3233	RAM3133 *btuB*::Tn*10*	This study
RAM3234	RAM3133 *btuB*::Tn*10 rpoB58*	This study
RAM3235	RAM3134 *btuB*::Tn*10*	This study
RAM3236	RAM3134 *btuB*::Tn*10 rpoB58*	This study
RAM3284	RAM2370 Δ*acrE*::scar	This study
RAM3285	RAM3284 *baeS51*	This study
RAM3286	RAM3284 *baeS52*	This study
RAM3287	RAM3284 *baeS59*	This study
RAM3288	RAM3284 *baeS61*	This study
RAM3289	RAM3284 *baeS63*	This study
RAM3290	RAM3284 *spy*::*lacZ* (Km^r)	This study
RAM3291	RAM3285 *spy*::*lacZ* (Km^r)	This study
RAM3292	RAM3286 *spy*::*lacZ* (Km^r)	This study
RAM3293	RAM3287 *spy*::*lacZ* (Km^r)	This study
RAM3294	RAM3288 *spy*::*lacZ* (Km^r)	This study
RAM3295	RAM3289 *spy*::*lacZ* (Km^r)	This study
RAM3296	RAM3284 *rpoB53*	This study
RAM3297	RAM3284 *rpoB55*	This study
RAM3298	RAM3284 *rpoB57*	This study
RAM3299	RAM3284 *rpoB58*	This study
RAM3300	RAM3299 *spy*::*lacZ* (Km^r)	This study
RAM3301	RAM1292 *btuB*::Tn*10 rpoB53*	This study
RAM3302	RAM1292 *btuB*::Tn*10 rpoB55*	This study
RAM3303	RAM1292 *btuB*::Tn*10 rpoB57*	This study
RAM3304	RAM3027 Δ*dksA*::Km^r	This study
RAM3305	RAM3301 Δ*dksA*::Km^r	This study
RAM3306	RAM3302 Δ*dksA*::Km^r	This study
RAM3307	RAM3303 Δ*dksA*::Km^r	This study
RAM3308	RAM3028 Δ*dksA*::Km^r	This study

RNA obtained from independent bacterial cultures. The adapter-ligated libraries were cleaned using AMPure beads (Agencourt Bioscience/Beckman Coulter; catalog no. A63883) and amplified with Kapa's HiFi enzyme (Kapa code KK2502). Each library was then analyzed for fragment size on an Agilent Tapestation and quantified by quantitative PCR (qPCR) (KAPA code KK4835) on Thermo Fisher Scientific's QuantStudio 5 before multiplex pooling and sequencing on a 2 by 75 flow cell on the NextSeq500 platform (Illumina) at the Arizona State University Genomics Core facility.

RNA-seq reads for each sample were quality checked using FastQC v0.10.1 and aligned to *Escherichia coli* K-12 MC4100 genome assembly from the NCBI database (GenBank Assembly accession no. GCF_000499485.1) using STAR v2.5.1b. A series of quality control metrics was generated on the STAR outputs. Cufflinks v2.2.1 was used to report FPKM values (fragments per kilobase of transcript per million mapped reads) and read counts. TPM (transcripts per million) was calculated by an in-house R script. Differential gene expression (DGE) analysis was performed with the EdgeR package from Bioconductor v3.2 in R 3.2.3. Multidimensional scaling (MSD) plot was drawn by plotMDS in which distances correspond to leading log fold changes between samples. EdgeR applied an overdispersed Poisson model to account for variance among biological replicates. Empirical Bayes tagwise dispersions are also estimated to moderate the overdispersion across transcripts. Then a negative binomial generalized log-linear model was fit to the read counts for each gene for all comparison pairs. For each pairwise comparison, genes with false-discovery rate (FDR) of <0.05 were considered significant, and $\log_2$ fold change of expression between conditions ($\log_2$ FC) was reported. FDR was calculated following Benjamini and Hochberg (82) procedure, the expected proportion of false discoveries among the rejected hypotheses.

Data availability. RNA-seq data sets were submitted to NCBI SRA with the accession numbers of PRJNA726737 for *baeS51* and PRJNA726740 for *rpoB58*.

SUPPLEMENTAL MATERIAL

Supplemental material is available online only.

SUPPLEMENTAL FILE 1, PDF file, 0.5 MB.

SUPPLEMENTAL FILE 2, XLSX file, 0.4 MB.
SUPPLEMENTAL FILE 3, XLSX file, 0.5 MB.

ACKNOWLEDGMENTS

We are grateful to Keilen Kelly and Melody Yeh for critical reading and helpful comments on the manuscript. We thank Richard Gourse, Wilma Ross, and Judah Rosner for providing *lacZ* fusion constructs. We also thank Shanshan Yang, Jason Steel, and their genomics team at the Arizona State University Core Research Facilities for whole-genome sequencing and RNA-seq analyses.

The work was funded by now-completed NIH grant R21 AI117150.

REFERENCES

1. Blanco P, Hernando-Amado S, Reales-Calderon JA, Corona F, Lira F, Alcalde-Rico M, Bernardini A, Sanchez MB, Martinez JL. 2016. Bacterial multidrug efflux pumps: much more than antibiotic resistance determinants. Microorganisms 4:14. https://doi.org/10.3390/microorganisms4010014.
2. Anes J, McCusker MP, Fanning S, Martins M. 2015. The ins and outs of RND efflux pumps in *Escherichia coli*. Front Microbiol 6:587. https://doi.org/10.3389/fmicb.2015.00587.
3. Pos KM. 2009. Drug transport mechanism of the AcrB efflux pump. Biochim Biophys Acta 1794:782–793. https://doi.org/10.1016/j.bbapap.2008.12.015.
4. Misra R, Bavro VN. 2009. Assembly and transport mechanism of drug efflux systems. Biochim Biophys Acta 1794:817–825. https://doi.org/10.1016/j.bbapap.2009.02.017.
5. Fralick JA, Burns-Keliher LL. 1994. Additive effect of *tolC* and *rfa* mutations on the hydrophobic barrier of the outer membrane of *Escherichia coli* K-12. J Bacteriol 176:6404–6406. https://doi.org/10.1128/JB.176.20.6404-6406.1994.
6. Koronakis V, Sharff A, Koronakis E, Luisi B, Hughes C. 2000. Crystal structure of the bacterial membrane protein TolC central to multidrug efflux and protein export. Nature 405:914–919. https://doi.org/10.1038/35016007.
7. Nishino K, Yamaguchi A. 2001. Analysis of a complete library of putative drug transporter genes in *Escherichia coli*. J Bacteriol 183:5803–5812. https://doi.org/10.1128/JB.183.20.5803-5812.2001.
8. Ma D, Cook DN, Alberti M, Pon NG, Nikaido H, Hearst JE. 1995. Genes *acrA* and *acrB* encode a stress-induced drug efflux system of *Escherichia coli*. Mol Microbiol 16:45–55. https://doi.org/10.1111/j.1365-2958.1995.tb02390.x.
9. Augustus AM, Celaya T, Husain F, Humbard M, Misra R. 2004. Antibiotic-sensitive TolC mutants and their suppressors. J Bacteriol 186:1851–1860. https://doi.org/10.1128/JB.186.6.1851-1860.2004.
10. Jellen-Ritter AS, Kern WV. 2001. Enhanced expression of the multidrug efflux pumps AcrAB and AcrEF associated with insertion element transposition in *Escherichia coli* mutants selected with a fluoroquinolone. Antimicrob Agents Chemother 45:1467–1472. https://doi.org/10.1128/AAC.45.5.1467-1472.2001.
11. Kobayashi K, Tsukagoshi N, Aono R. 2001. Suppression of hypersensitivity of *Escherichia coli acrB* mutant to organic solvents by integrational activation of the *acrEF* operon with the IS*1* or IS*2* element. J Bacteriol 183:2646–2653. https://doi.org/10.1128/JB.183.8.2646-2653.2001.
12. Misra R, Morrison KD, Cho HJ, Khuu T. 2015. Importance of real-time assays to distinguish multidrug efflux pump-inhibiting and outer membrane-destabilizing activities in *Escherichia coli*. J Bacteriol 197:2479–2488. https://doi.org/10.1128/JB.02456-14.
13. Nagakubo S, Nishino K, Hirata T, Yamaguchi A. 2002. The putative response regulator BaeR stimulates multidrug resistance of *Escherichia coli* via a novel multidrug exporter system, MdtABC. J Bacteriol 184:4161–4167. https://doi.org/10.1128/JB.184.15.4161-4167.2002.
14. Ma D, Alberti M, Lynch C, Nikaido H, Hearst JE. 1996. The local repressor AcrR plays a modulating role in the regulation of *acrAB* genes of *Escherichia coli* by global stress signals. Mol Microbiol 19:101–112. https://doi.org/10.1046/j.1365-2958.1996.357881.x.
15. Hirakawa H, Takumi-Kobayashi A, Theisen U, Hirata T, Nishino K, Yamaguchi A. 2008. AcrS/EnvR represses expression of the *acrAB* efflux genes in *Escherichia coli*. J Bacteriol 190:6276–6279. https://doi.org/10.1128/JB.00190-08.
16. Rosenberg EY, Bertenthal D, Nilles ML, Bertrand KP, Nikaido H. 2003. Bile salts and fatty acids induce the expression of *Escherichia coli* AcrAB multidrug efflux pump through their interaction with Rob regulatory protein. Mol Microbiol 48:1609–1619. https://doi.org/10.1046/j.1365-2958.2003.03531.x.
17. Grainger DC. 2016. Structure and function of bacterial H-NS protein. Biochem Soc Transac 44:1561–1569. https://doi.org/10.1042/BST20160190.
18. Nishino K, Yamaguchi A. 2004. Role of histone-like protein H-NS in multidrug resistance of *Escherichia coli*. J Bacteriol 186:1423–1429. https://doi.org/10.1128/JB.186.5.1423-1429.2004.
19. Nishino K, Senda Y, Yamaguchi A. 2008. CRP regulator modulates multidrug resistance of *Escherichia coli* by repressing the *mdtEF* multidrug efflux genes. J Antibiot 61:120–127. https://doi.org/10.1038/ja.2008.120.
20. Baranova N, Nikaido H. 2002. The BaeSR two-component regulatory system activates transcription of the *yegMNOB* (*mdtABCD*) transporter gene cluster in *Escherichia coli* and increases its resistance to novobiocin and deoxycholate. J Bacteriol 184:4168–4176. https://doi.org/10.1128/JB.184.15.4168-4176.2002.
21. Pagès J-M, Muriel M, Barbe J. 2005. Inhibitors of efflux pumps in Gram-negative bacteria. Trends Mol Med 11:382–389. https://doi.org/10.1016/j.molmed.2005.06.006.
22. Bambeke FV, Pagès J-M, Lee VJ. 2010. Inhibitors of bacterial efflux pumps as adjuvants in antibacterial therapy and diagnostic tools for detection of resistance by efflux, p 138–175. *In* Atta-ur-Rahman, Choudhary MI (ed), Frontiers in anti-infective drug discovery, vol. 1. Bentham Science Publishers, Sharjah, United Arab Emirates.
23. Spengler G, Kincses A, Gajdács M, Amaral L. 2017. New roads leading to old destination: efflux pumps as targets to reverse multidrug resistance in bacteria. Molecules 22:468. https://doi.org/10.3390/molecules22030468.
24. Blair JMA, Webber MA, Baylay AJ, Ogbolu DO, Piddock LJV. 2015. Molecular mechanisms of antibiotic resistance. Nat Rev Microbiol 13:42–51. https://doi.org/10.1038/nrmicro3380.
25. Munita JM, Arias JA. 2016. Mechanisms of antibiotic resistance. Microbiol Spectr 4:1–24. https://doi.org/10.1128/microbiolspec.VMBF-0016-2015.
26. Delcour AH. 2009. Outer membrane permeability and antibiotic resistance. Biochim Biophys Acta 1794:808–816. https://doi.org/10.1016/j.bbapap.2008.11.005.
27. Cabral DJ, Wurster JI, Belenky P. 2018. Antibiotic persistence as a metabolic adaptation: stress, metabolism, the host, and new direction. Pharmaceuticals 11:14. https://doi.org/10.3390/ph11010014.
28. Sjuts H, Vargiu AV, Kwasny SM, Nguyen ST, Kim H-S, Ding X, Ornik AR, Ruggerone P, Bowlin TL, Nikaido H, Pos KM, Opperman TJ. 2016. Molecular basis for inhibition AcrB multidrug efflux pump by novel and powerful pyranopyridine derivatives. Proc Natl Acad Sci U S A 113:3509–3514. https://doi.org/10.1073/pnas.1602472113.
29. Cudkowicz NA, Schuldiner S. 2019. Deletion of the major *Escherichia coli* multidrug efflux transporter AcrB reveals transporter plasticity and redundancy in bacterial cells. PLoS One 14:e0218828. https://doi.org/10.1371/journal.pone.0218828.
30. Gross CH, Parsons JD, Grossman TH, Charifson PS, Bellon S, Jernee J, Dwyer M, Chambers SP, Markland W, Botfield M, Raybuck SA. 2003. Active-site residues of *Escherichia coli* DNA gyrase required in coupling ATP hydrolysis to DNA supercoiling and amino acid substitutions leading to novobiocin resistance. Antimicrob Agents Chemother 47:1037–1046. https://doi.org/10.1128/AAC.47.3.1037-1046.2003.
31. Hardy CD, Cozzarelli NR. 2003. Alteration of topoisomerase IV to novobiocin resistance. Antimicrob Agents Chemother 47:941–947. https://doi.org/10.1128/AAC.47.3.941-947.2003.

32. Gaynor M, Mankin AS. 2003. Macrolide antibiotics: binding sites, mechanism of action, resistance. Curr Top Med Chem 3:949–961. https://doi.org/10.2174/1568026033452159.
33. Sigmund CD, Morgan EA. 1982. Erythromycin resistance due to a mutation in the ribosomal RNA operon in *Escherichia coli*. Proc Natl Acad Sci U S A 79:5602–5606. https://doi.org/10.1073/pnas.79.18.5602.
34. Ettayebi M, Prasad SM, Morgan EA. 1985. Chloramphenicol-erythromycin resistance mutation in a 23S rRNA gene of *Escherichia coli*. J Bacterial 162:551–557. https://doi.org/10.1128/JB.162.2.551-557.1985.
35. Chittum HS, Champney WS. 1994. Ribosomal protein gene sequences changes in erythromycin-resistant mutants of *Escherichia coli*. J Bacteriol 176:6192–6198. https://doi.org/10.1128/JB.176.20.6192-6198.1994.
36. Hazelbauer-Randall L, Schwartz M. 1973. Isolation of the bacteriophage lambda receptor from *Escherichia coli*. J Bacteriol 116:1436–1446. https://doi.org/10.1128/JB.116.3.1436-1446.1973.
37. Boos W, Shuman H. 1998. Maltose/maltodextrin system of *Escherichia coli*: transport, metabolism, and regulation. Microbiol Mol Biol Rev 62:204–229. https://doi.org/10.1128/MMBR.62.1.204-229.1998.
38. Williams RM, Rimsky S, Buc H. 1996. Probing the structure, function, and interactions of *Escherichia coli* H-NS and StpA proteins by using dominant negative derivatives. J Bacteriol 178:4335–4343. https://doi.org/10.1128/JB.178.15.4335-4343.1996.
39. Ueguchi C, Seto C, Suzuki T, Mizuno T. 1997. Clarification of the dimerization domain and its functional significance for the *Escherichia coli* nucleoid protein H-NS. J Mol Biol 274:145–151. https://doi.org/10.1006/jmbi.1997.1381.
40. Kim H-S, Nagore D, Nikaido H. 2010. Multidrug efflux pump MdtBC of *Escherichia coli* is active only as a B_2C heterotrimer. J Bacteriol 192:1377–1386. https://doi.org/10.1128/JB.01448-09.
41. Kim H-S, Nikaido H. 2012. Different functions of MdtB and MdtC subunits in the heterotrimeric efflux transporter $MdtB_2C$ complex of *Escherichia coli*. Biochem 51:4188–4197. https://doi.org/10.1021/bi300379y.
42. Raffa RG, Raivio TL. 2002. A third envelope stress signal transduction pathway in *Escherichia coli*. Mol Microbiol 45:1599–1611. https://doi.org/10.1046/j.1365-2958.2002.03112.x.
43. Hirakawa H, Inazumi Y, Masaki T, Hirata T, Yamaguchi A. 2004. Indole induces the expression of multidrug exporter genes in *Escherichia coli*. Mol Micobiol 55:1113–1126. https://doi.org/10.1111/j.1365-2958.2004.04449.x.
44. Nishino K, Nikaido E, Yamaguchi A. 2007. Regulation of multidrug efflux systems involved in multidrug and metal resistance of *Salmonella* enterica serovar Typhimurium. J Bacteriol 189:9066–9075. https://doi.org/10.1128/JB.01045-07.
45. Appia-Ayme C, Patric E, Sullivan MJ, Alston MJ, Field SJ, AbuOun M, Anjum MF, Rowley G. 2011. Novel inducers of the envelope stress response BaeSR in *Salmonella* Typhimurium: BaeR is critically required for tungstate waste disposal. PLoS One 6:e23713. https://doi.org/10.1371/journal.pone.0023713.
46. Leblanc SKD, Oates CW, Raivio TL. 2011. Characterization of the induction and cellular role of the BaeSR two-component envelope stress response of *Escherichia coli*. J Bacteriol 193:3367–3375. https://doi.org/10.1128/JB.01534-10.
47. Wang D, Fierke CA. 2013. The BaeSR regulon is involved in defense against zinc toxicity in *E. coli*. Metallomics 5:372–383. https://doi.org/10.1039/c3mt20217h.
48. Srivastava SK, Lambadi PR, Ghosh T, Pathania R, Navani NK. 2014. Genetic regulation of *spy* gene expression in *Escherichia coli* in the presence of protein unfolding agent ethanol. Gene 548:142–148. https://doi.org/10.1016/j.gene.2014.07.003.
49. Nishino K, Honda T, Yamaguchi A. 2005. Genome-wide analyses of *Escherichia coli* gene expression responsive to the BaeSR two-component regulatory system. J Bacteriol 187:1763–1772. https://doi.org/10.1128/JB.187.5.1763-1772.2005.
50. Rosner JL, Martin RG. 2013. Reduction of cellular stress by TolC-dependent efflux pumps in *Escherichia coli* indicated by BaeSR and CpxARP activation of *spy* in efflux mutants. J Bacteriol 195:1042–1050. https://doi.org/10.1128/JB.01996-12.
51. Choudhary KS, Kleinmanns JA, Decker K, Sastry AV, Gao Y, Szubin R, Seif Y, Palsson BO. 2020. Elucidation of regulatory modes for five two-component systems in *Escherichia coli* reveals novel relationships. mSystems 5:e00980-20. https://doi.org/10.1128/mSystems.00980-20.
52. Aires JR, Nikaido H. 2005. Aminoglycosides are captured from both periplasm and cytoplasm by the AcrD multidrug efflux transporter of *Escherichia coli*. J Bacteriol 187:1923–1929. https://doi.org/10.1128/JB.187.6.1923-1929.2005.
53. Datsenko KA, Wanner BL. 2000. One-step inactivation of chromosomal genes in *Escherichia coli* K-12 using PCR products. Proc Natl Acad Sci U S A 97:6640–6645. https://doi.org/10.1073/pnas.120163297.
54. Frawley ER, Crouch M-LV, Bingham-Ramos LK, Robbins HF, Wang E, Wright GD, Fang FC. 2013. Iron and citrate export by a major facilitator superfamily pump regulates metabolism and stress resistance in *Salmonella* Typhimurium. Proc Natl Acad Sci U S A 110:12054–12059. https://doi.org/10.1073/pnas.1218274110.
55. Model P, Jovanovic G, Dworkin J. 1997. The *Escherichia coli* phage-shock-protein (*psp*) operon. Mol Microbiol 24:255–261. https://doi.org/10.1046/j.1365-2958.1997.3481712.x.
56. Hartmann G, Honikel KO, Knüsel F, Nüesch J. 1967. The specific inhibition of the DNA-directed RNA synthesis by rifamycin. Biochim Biophys Acta 145:843–844. https://doi.org/10.1016/0005-2787(67)90147-5.
57. Wehrli W. 1983. Rifampin: mechanisms of action and resistance. Rev Infect Dis 5:S407–S411. https://doi.org/10.1093/clinids/5.Supplement_3.S407.
58. Jin DJ, Gross CA. 1988. Mapping and sequencing of mutations in the *Escherichia coli rpoB* gene that lead to rifampin resistance. J Mol Biol 202:45–58. https://doi.org/10.1016/0022-2836(88)90517-7.
59. Pietsch F, Bergman JM, Brandis G, Marcusson LL, Zorzet A, Huseby DL, Hughes D. 2017. Ciprofloxacin selects for RNA polymerase mutations and pleiotropic antibiotic resistance effects. J Antimicrob Chemother 72:75–84. https://doi.org/10.1093/jac/dkw364.
60. Sanchez-Vazquez P, Dewey CN, Kitten N, Ross W, Gourse RL. 2019. Genome-wide effects on *Escherichia coli* transcription from ppGpp binding to its two sites on RNA polymerase. Proc Natl Acad Sci U S A 116:8310–8319. https://doi.org/10.1073/pnas.1819682116.
61. Cashel M, Gallant J. 1969. Two compounds implicated in the function of *RC* gene of *Escherichia coli*. Nature 221:838–841. https://doi.org/10.1038/221838a0.
62. Haseltine WA, Block R. 1973. Synthesis of guanosine tetra- and pentaphosphate requires the presence of a codon-specific, uncharged transfer ribonucleic acid in the acceptor site of ribosomes. Proc Natl Acad Sci U S A 70:1564–1568. https://doi.org/10.1073/pnas.70.5.1564.
63. Ross W, Sanchez-Vazquez P, Chen AY, Lee J-H, Burgos HL, Gourse RL. 2016. ppGpp binding to a site at the RNAP-DksA interface accounts for its dramatic effects on transcription initiation during the stringent response. Mol Cell 62:811–823. https://doi.org/10.1016/j.molcel.2016.04.029.
64. Loewen PC, Hengge-Aronis R. 1994. The role of the sigma factor σ^S (KatF) in bacterial global regulation. Annu Rev Microbiol 48:53–80. https://doi.org/10.1146/annurev.mi.48.100194.000413.
65. Weber H, Polen T, Heuveling J, Wendisch VF, Hengge R. 2005. Genome-wide analysis of the general stress response network in *Escherichia coli*: σ^S-dependent genes, promoters, and sigma factor selectively. J Bacteriol 187:1591–1603. https://doi.org/10.1128/JB.187.5.1591-1603.2005.
66. Greenway DLA, England RR. 1999. The intrinsic resistance of *Escherichia coli* to various antimicrobial agents requires ppGpp and σ^S. Lett Appl Microbiol 29:323–326. https://doi.org/10.1046/j.1472-765X.1999.00642.x.
67. Hobbs JK, Boraston AB. 2019. (p)ppGpp and the stringent response: an emerging target to antibiotic therapy. ACS Infect Dis 5:1505–1517. https://doi.org/10.1021/acsinfecdis.9b00204.
68. Nguyen D, Joshi-Datar A, Lepine F, Bauerle E, Olakanmi O, Beer K, McKay G, Siehnel R, Schafhauser J, Wang Y, Britigan BE, Singh PK. 2011. Active starvation responses mediate antibiotic tolerance in biofilms and nutrient-limited bacteria. Science 334:982–986. https://doi.org/10.1126/science.1211037.
69. Zhou YN, Jin DJ. 1998. The *rpoB* mutants destabilizing initiation complexes at stringently controlled promoters behave like "stringent" RNA polymerases in *Escherichia coli*. Proc Natl Acad Sci U S A95:2908–2913. https://doi.org/10.1073/pnas.95.6.2908.
70. Gourse RL, Chen AY, Gopalkrishnan S, Sanchez-Vazquez P, Myers A, Ross R. 2018. Transcriptional response to ppGpp and DksA. Annu Rev Microbiol 72:163–184. https://doi.org/10.1146/annurev-micro-090817-062444.
71. Parshin A, Shiver AL, Lee J, Ozerova M, Schneidman-Duhovny D, Gross CA, Borukhov S. 2015. DksA regulates RNA polymerase in *Escherichia coli* through a network of interactions in the secondary channel that includes sequence insertion 1. Proc Natl Acad Sci U S A 112:E6862–E6871. https://doi.org/10.1073/pnas.1521365112.
72. Brown L, Gentry D, Elliot T, Cashel M. 2002. DksA affects ppGpp induction of RpoS at a translational level. J Bacteriol 184:4455–4465. https://doi.org/10.1128/JB.184.16.4455-4465.2002.

73. Magnusson LU, Gummesson B, Joksimović P, Farewell A, Nyström T. 2007. Identical, independent, and opposing roles of ppGpp and DksA in *Escherichia coli*. J Bacteriol 189:5193–5202. https://doi.org/10.1128/JB.00330-07.
74. Paul BJ, Berkmen MB, Gourse RL. 2005. DksA potentiates direct activation of amino acid promoters by ppGpp. Proc Natl Acad Sci U S A 102:7823–7828. https://doi.org/10.1073/pnas.0501170102.
75. Rutherford ST, Villers CL, Lee J-H, Ross W, Gourse RL. 2009. Allosteric control of *Escherichia coli* rRNA promoter complexes by DksA. Genes Dev 23:236–248. https://doi.org/10.1101/gad.1745409.
76. Wang J, Cao L, Yang X, Wu Q, Lu L, Wang Z. 2018. Transcriptional analysis reveals the critical role of RNA polymerase-binding transcription factor, DksA, in regulating multi-drug resistance in *Escherichia coli*. Int J Antimicrob Agents 52:63–69. https://doi.org/10.1016/j.ijantimicag.2018.05.002.
77. Honsa ES, Cooper VS, Mhaissen MN, Frank M, Shaker J, Iverson A, Rubnitz J, Hayden RT, Lee RE, Rock CO, Tuomanen EI, Wolf J, Rosch JW. 2017. RelA mutant *Enterococcus faecium* with multiantibiotic tolerance arising in an immunocompromised host. mBio 8:e02124-16. https://doi.org/10.1128/mBio.02124-16.
78. Pool K. 2012. Bacterial stress responses as determinants of antimicrobial resistance. J Antimicrob Chemother 67:2069–2089. https://doi.org/10.1093/jac/dks196.
79. Werner J, Misra R. 2005. YaeT (Omp85) affects the assembly of lipid-dependent and lipid independent outer membrane proteins of *Escherichia coli*. Mol Microbiol 57:1450–1459. https://doi.org/10.1111/j.1365-2958.2005.04775.x.
80. Silhavy TJ, Berman ML, Enquist LW. 1984. Experiments with gene fusions. Cold Spring Harbor Laboratory Press, Cold Spring Harbor, NY.
81. Miller JH. 1992. A short course in bacterial genetics: a laboratory manual and handbook for Escherichia coli and related bacteria, p 71–74. Cold Spring Harbor Laboratory Press, Cold Spring Harbor, NY.
82. Benjamini Y, Hochberg Y. 1995. Controlling the false discovery rate: a practical and powerful approach to multiple testing. J R Statist Soc B Series 57:289–300. https://doi.org/10.1111/j.2517-6161.1995.tb02031.x.
83. Barker MM, Gaal T, Josaitis CA, Gourse RL. 2001. Mechanism of regulation of transcription initiation by ppGpp. I. Effects of ppGpp on transcription initiation *in vivo* and *in vitro*. J Mol Biol 305:673–688. https://doi.org/10.1006/jmbi.2000.4327.